Irradiation intensity dependent heterogeneous formation of sulfate and dissolution of ZnO nanoparticles

Tao Wang[1], Yangyang Liu[1], Yue Deng[1], Hanyun Cheng[1], Yang Yang[1], Kejian Li[1], Xiaozhong Fang[1], Liwu Zhang[1,2*]

[1] Shanghai Key Laboratory of Atmospheric Particle Pollution and Prevention, Department of Environmental Science & Engineering, Fudan University, Shanghai, 200433, Peoples' Republic of China

[2] Shanghai Institute of Pollution Control and Ecological Security, Shanghai, 200092, Peoples' Republic of China

Number of Pages: 8

Number of Figures: 7

Number of Tables: 2

Number of Reactions: 24

Catalogue

Section S1. Experimental

In-situ diffuse reflectance infrared Fourier transform spectroscopy (DRIFTS) is helpful in discussing the species formed on particles. The schematic diagram of the in-situ setup is present in **Figure S1**. ZnO particles were placed in a ceramic sample cup (0.35 mm depth, 5 mm i.d.). Mass flow controllers (Beijing Sevenstar electronics Co., LTD) were used to adjust the fluxes of reactant gases to the desired flow rate, concentration and relative humidity (RH). A temperature controller was connected to the DRIFTS chamber (Praying Mantis Kit, Harrick) to control the reaction temperature (298 K).

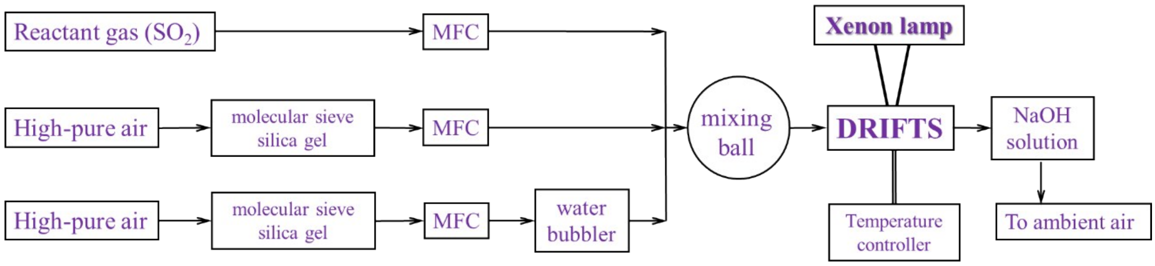

Figure S1. Schematic diagram of experimental setup. The DRIFTS chamber is linked with other parts through Teflon tube. MFC: mass flow controller

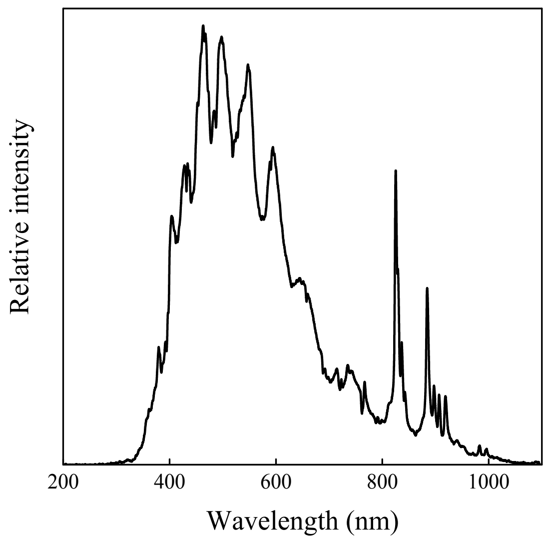

Figure S2. Spectral distribution of the Xenon lamp light measured by a fiber optic spectrometer (AULTT-P4000, Beijing Ceaulight Co., LTD, China).

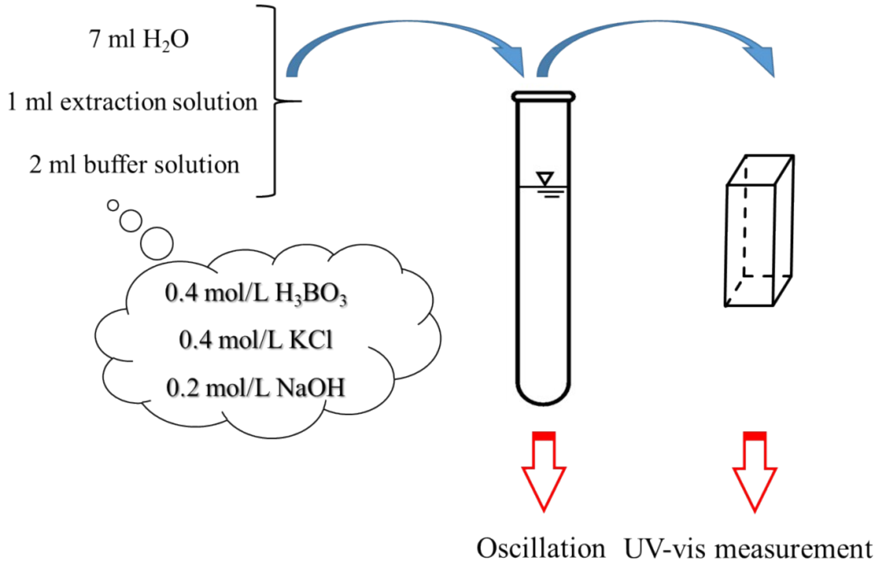

Figure S3. Process of the Zn^{2+} analysis by means of UV-vis.

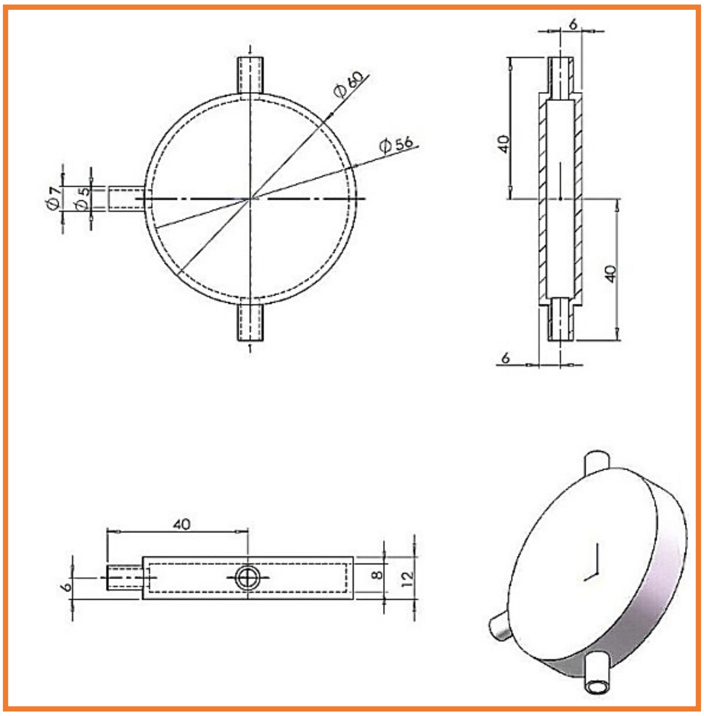

Figure S4. Reactor for the ex-situ experiments.

Section S2. Kinetics evaluation

In the estimation of the uptake coefficients, both BET surface area (A_{BET}) and geometric surface area (A_{geo}) are adopted as the reactive surface area (A_s). If the reaction probability is high, the reactants would have no time to diffuse into the sample and the A_s thus be the geometric surface area of the sample cup (A_{geo}). On the contrary, A_{BET}, calculated based on S_{BET} and particle mass (A_{BET}= S_{BET}×mass), would more appropriately represent A_s when the reaction probability is low and the reactants may have enough time to diffuse into the entire sample. Hence, γ-values estimated via A_{BET} and A_{geo} (denoted as γ_{BET} and γ_{geo}, respectively) are mentioned simultaneously to represent the lower and upper limits of γ-values varying with reaction probabilities between the reactants and particles.

Table S1. Parameters for uptake coefficient estimations.

Parameter (unit)		Value
Sulfate formation rate: $d[SO_4^{2-}]/dt$ (ion·s^{-1})		According to reactions
Particle reactive surface area: As (m^2)	A_{BET} (m^2)	S_{BET} × sample mass
	A_{geo} (m^2)	1.86×10^{-5}
Reactant concentration: [SO_2] (molecule·m^{-3})		3.773×10^{20}
Velocity of molecule: v_{SO_2}	Gas constant: R (J·mol^{-1}·K^{-1})	8.314
	Temperature: T (Kelvin)	298
	Molar mass: M_{SO_2} (kg·mol^{-1})	64.06
	Pi: π (dimensionless)	3.1416

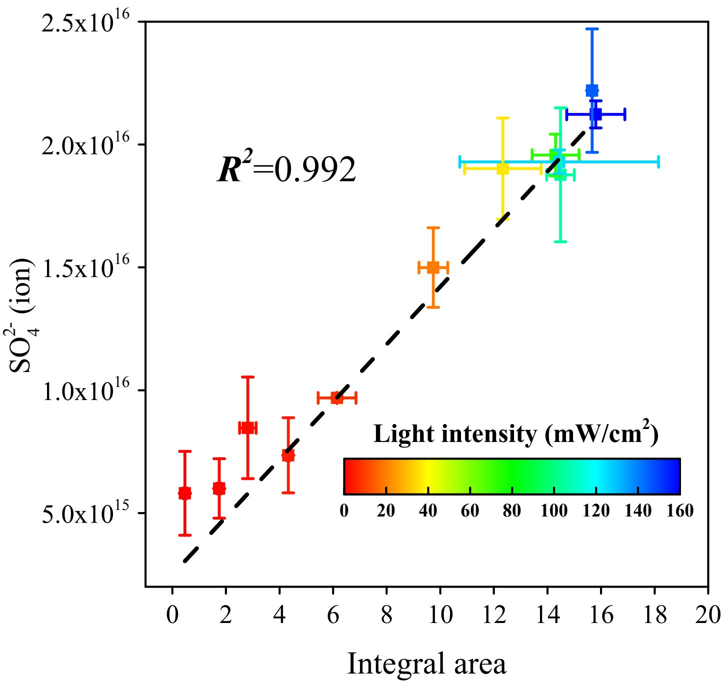

Figure S5. Calibration plot with amount of SO_4^{2-} versus corresponding integrated areas for sulfate species.

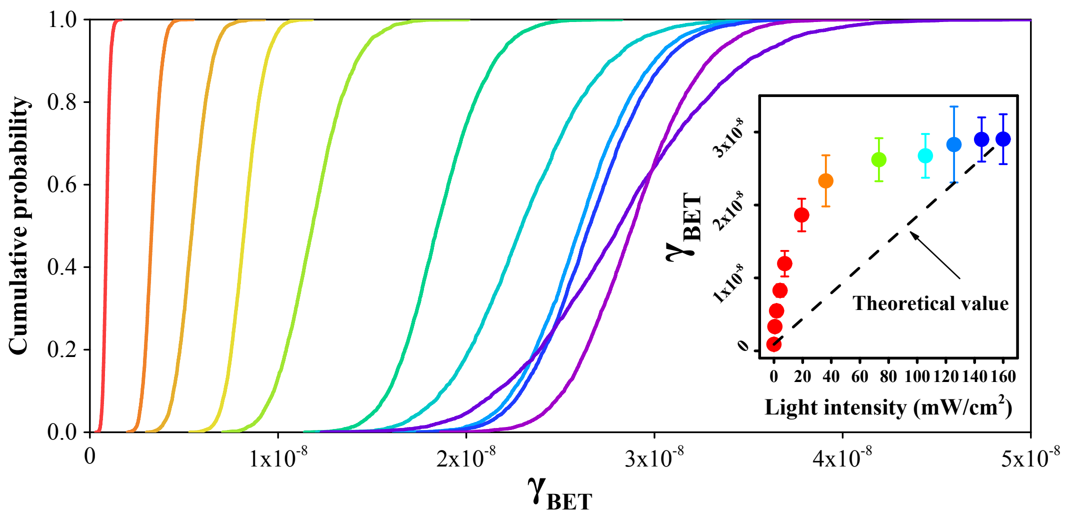

Figure S6. Cumulative probability of the γ_{BET} values based on Monte Carlo simulation. Inset: actual γ-values (Mean±1σ) and theoretical ones.

Table S2. Reactive uptake coefficients (γ_{BET} and γ_{geo}) for the heterogeneous uptake of SO_2 on particles under various light intensities.

Light intensity	γ_{BET}						γ_{geo}					
($mW\cdot cm^{-2}$)	10th	25th	50th	75th	90th	Mean±SD	10th	25th	50th	75th	90th	Mean±SD
0.0	6.83×10^{-10}	7.73×10^{-10}	8.85×10^{-10}	9.93×10^{-10}	1.10×10^{-9}	$8.90\times10^{-10}\pm1.68\times10^{-10}$	3.83×10^{-6}	4.34×10^{-6}	4.92×10^{-6}	5.48×10^{-6}	6.07×10^{-6}	$4.94\times10^{-6}\pm8.74\times10^{-7}$
0.71	2.78×10^{-9}	3.02×10^{-9}	3.29×10^{-9}	3.59×10^{-9}	3.86×10^{-9}	$3.32\times10^{-9}\pm4.18\times10^{-10}$	1.58×10^{-5}	1.70×10^{-5}	1.83×10^{-5}	1.97×10^{-5}	2.10×10^{-5}	$1.84\times10^{-5}\pm2.03\times10^{-6}$
1.86	4.44×10^{-9}	4.91×10^{-9}	5.44×10^{-9}	6.00×10^{-9}	6.53×10^{-9}	$5.48\times10^{-9}\pm8.16\times10^{-10}$	2.51×10^{-5}	2.75×10^{-5}	3.02×10^{-5}	3.31×10^{-5}	3.57×10^{-5}	$3.05\times10^{-5}\pm4.14\times10^{-6}$
4.30	7.18×10^{-9}	7.65×10^{-9}	8.23×10^{-9}	8.81×10^{-9}	9.37×10^{-9}	$8.27\times10^{-9}\pm8.65\times10^{-10}$	4.08×10^{-5}	4.31×10^{-5}	4.58×10^{-5}	4.84×10^{-5}	5.08×10^{-5}	$4.59\times10^{-5}\pm3.94\times10^{-6}$
7.50	9.78×10^{-9}	1.07×10^{-8}	1.18×10^{-8}	1.30×10^{-8}	1.42×10^{-8}	$1.20\times10^{-8}\pm1.75\times10^{-9}$	5.51×10^{-5}	6.01×10^{-5}	6.58×10^{-5}	7.18×10^{-5}	7.74×10^{-5}	$6.62\times10^{-5}\pm8.73\times10^{-6}$
19.4	1.59×10^{-8}	1.71×10^{-8}	1.85×10^{-8}	2.00×10^{-8}	2.15×10^{-8}	$1.86\times10^{-8}\pm2.23\times10^{-9}$	8.98×10^{-5}	9.60×10^{-5}	1.03×10^{-4}	1.10×10^{-4}	1.17×10^{-4}	$1.03\times10^{-4}\pm1.08\times10^{-5}$
36.2	1.88×10^{-8}	2.07×10^{-8}	2.30×10^{-8}	2.54×10^{-8}	2.77×10^{-8}	$2.33\times10^{-8}\pm3.51\times10^{-9}$	1.06×10^{-4}	1.17×10^{-4}	1.28×10^{-4}	1.40×10^{-4}	1.52×10^{-4}	$1.29\times10^{-4}\pm1.78\times10^{-5}$
73.3	2.25×10^{-8}	2.41×10^{-8}	2.61×10^{-8}	2.81×10^{-8}	3.00×10^{-8}	$2.62\times10^{-8}\pm2.95\times10^{-9}$	1.27×10^{-4}	1.36×10^{-4}	1.50×10^{-4}	1.54×10^{-4}	1.63×10^{-4}	$1.45\times10^{-4}\pm1.39\times10^{-5}$
105.7	2.29×10^{-8}	2.47×10^{-8}	2.66×10^{-8}	2.87×10^{-8}	3.06×10^{-8}	$2.67\times10^{-8}\pm3.00\times10^{-9}$	1.30×10^{-4}	1.38×10^{-4}	1.48×10^{-4}	1.57×10^{-4}	1.66×10^{-4}	$1.49\times10^{-4}\pm1.42\times10^{-5}$
125.7	2.16×10^{-8}	2.47×10^{-8}	2.81×10^{-8}	3.16×10^{-8}	3.50×10^{-8}	$2.83\times10^{-8}\pm5.21\times10^{-9}$	1.22×10^{-4}	1.38×10^{-4}	1.57×10^{-4}	1.75×10^{-4}	1.92×10^{-4}	$1.58\times10^{-4}\pm2.74\times10^{-5}$
145	2.52×10^{-8}	2.68×10^{-8}	2.89×10^{-8}	3.09×10^{-08}	3.29×10^{-8}	$2.90\times10^{-8}\pm3.03\times10^{-9}$	1.43×10^{-4}	1.51×10^{-4}	1.61×10^{-4}	1.70×10^{-4}	1.78×10^{-4}	$1.61\times10^{-4}\pm1.38\times10^{-5}$
160	2.48×10^{-8}	2.66×10^{-8}	2.88×10^{-8}	3.12×10^{-08}	3.35×10^{-8}	$2.90\times10^{-8}\pm3.42\times10^{-9}$	1.40×10^{-4}	1.50×10^{-4}	1.60×10^{-4}	1.72×10^{-4}	1.82×10^{-4}	$1.61\times10^{-4}\pm1.65\times10^{-5}$

Section S3. XPS evidence

S (IV) and S(VI) species can be distinguished according to the analysis on the XPS spectra for pure $ZnSO_4$ and $ZnSO_3$ **(Figure S7)**, The S(Ⅳ) species were observed at 166.8 and 167.9 eV for the $S2p_{3/2}$ and $S2p_{1/2}$ transitions, respectively. Correspondingly, the S(Ⅵ) ones characterized by $S2p_{3/2}$ and $S2p_{1/2}$ transitions could be identified at 169.0 and 170.0 eV, respectively.

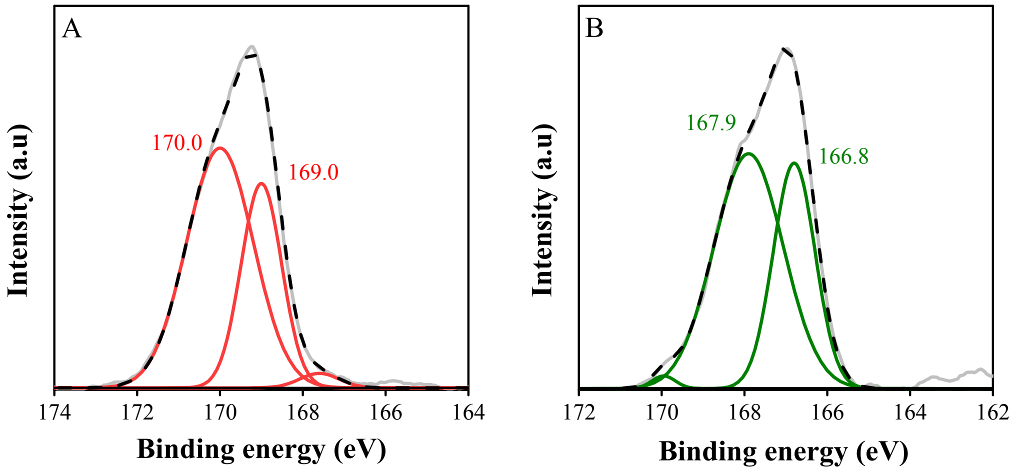

Figure S7. High resolution XPS data in the S2p regions for (A) $ZnSO_4$ and (B) $ZnSO_3$.

Section S4. Detailed reactions in the photocatalytic process

Reactions for the heterogeneous reaction of SO_2 on mineral dust particles are listed below according to some previous studies.

$SO_2(g) \leftrightharpoons SO_2(ads)$ R.(S1)

$SO_2 + O^{2-}(lattice) \rightarrow SO_3^{2-}$ R.(S2)

$SO_2 + 2OH^- \rightarrow SO_3^{2-} + H_2O$ R.(S3)

$SO_2 + OH^- \rightarrow HSO_3^-$ R.(S4)

$O_2 + e^- \xrightarrow{O(vacancy)} O_2^-(ads)$ R.(S5)

$O_2^-(ads) + e^- \rightarrow 2O^-(ads)$ R.(S6)

$SO_3^{2-} + O^- \rightarrow SO_4^{2-} + e^-$ R.(S7)

$SO_2 + H_2O \leftrightharpoons SO_2 \cdot H_2O \leftrightharpoons H_2SO_3$ R.(S8)

$H_2SO_3 \leftrightharpoons HSO_3^- + H^+$ R.(S9)

$HSO_3^- \leftrightharpoons SO_3^{2-} + H^+$ R.(S10)

$HSO_3^- + OH^- \leftrightharpoons SO_3^{2-} + H_2O$ R.(S11)

$HSO_3^- + O^- \leftrightharpoons HSO_4^- + e^-$ R.(S12)

$SO_3^{2-} + O^- \rightarrow SO_4^{2-} + e^-$ R.(S13)

$HSO_3^- + \frac{1}{2}O_2 \leftrightharpoons HSO_4^-$ R.(S14)

$SO_3^{2-} + \frac{1}{2}O_2 \rightarrow SO_4^{2-}$ R.(S15)

$ZnO + hv(\lambda \leq 380nm) \rightarrow h^+ + e^-$ R.(S16)

$h^+ + H_2O \rightarrow H^+ + {}^{\cdot}OH$ R.(S17)

$e^- + O_2 \rightarrow O_2^{\cdot -}$ R.(S18)

$e^- + O_2 + H^+ \rightarrow HO_2^{\cdot}$ R.(S19)

$2h^+ + 2H_2O \rightarrow H_2O_2 + 2H^+$ R.(S20)

$2O_2^{\cdot -} + 2H^+ \rightarrow H_2O_2 + O_2$ R.(S21)

$H_2O_2 + hv \rightarrow 2{}^{\cdot}OH$ R.(S22)

$SO_3^{2-} + H^+ \leftrightharpoons HSO_3^-$ R.(S23)

$SO_4^{2-} + H^+ \leftrightharpoons HSO_4^-$ R.(S24)